

ADVANCED – STRAIN – HARDENING – APPROACH

Constitutive model for rock salt , describing transient, stationary, and
accelerated creep and dilatancy

EXTENDED SUMMARY

RALF-MICHAEL GÜNTHER

Introduction

It is well known that salt rock responds to loading by elastic and visco-plastic deformation. The stress-deformation behaviour which is characterized by time-dependent ductile deformation without any visible macroscopic fracture is denoted as creep. Creep tests under constant stress conditions reveal that in general creep may be subdivided into the following three phases:

1. Primary creep – also denoted as transient or non-stationary creep,
2. Secondary or stationary creep, and
3. Tertiary creep or creep failure.

These three phases of creep are in a close relation one with the others, and as a result of intracrystalline deformation processes they pass from one to the other. Primary creep is characterized by high deformation rates. Decisive causes for primary creep are the dislocations which are present within the lattice structure and which start to move when stress increases. With growing deformation, the motion capacity of the present dislocations diminishes. If deformation continues, new dislocations will be produced within the lattice. Thus, the density of dislocations rises, and this rising density will cause an increasing resistance against deformation itself so that for maintaining a constant deformation rate an increasingly higher force is necessary or the deformation rate will decrease even when load is kept constant. This material hardening which increases with increasing deformation is counteracted by the recovery of dislocations. Out of this process, stationary creep develops by the fact that formation rate and recovery rate tend to approach equal values. In this phase of creep the density of dislocations, the deformation resistance and consequently also the creep

rates devolve to constants (Blum 1978). When damaging processes and the softening processes which are linked to them and which start in the stress space above the dilatancy threshold (Hunsche 1998) achieve a critical value, creep will pass into its tertiary phase so that we can observe creep failure.

Here, a constitutive model is presented which is based on these physical processes and which describes all three creep phases in the scope of a creep model. In the present report, the theoretical considerations are illustrated together with the derivation of the corresponding parameters of the constitutive law for two Stassfurt rock salt varieties taken from the Sondershausen mine and the Asse site and with numerical recalculations of the respective laboratory tests. These numerical calculations were carried out with the explicit finite difference program FLAC (Itasca 2000) into which the constitutive model has been implemented as DLL file.

Damage-free creep

According to the strain-hardening theory (ODQVIST & HULT, 1962), on which that constitutive model is based the total strain consists of an elastic part and a creep part, which are described with following formulations:

$$\begin{aligned}\dot{\varepsilon}_{ij} &= \dot{\varepsilon}_{ij}^{el} + \dot{\varepsilon}_{ij}^{cr} \\ \dot{\varepsilon}_{ij}^{el} &= -\nu/E \dot{\sigma}_{kk} \delta_{ij} + (1+\nu)/E \dot{\sigma}_{kk} \\ \dot{\varepsilon}_{ij}^{cr} &= 3/2 \dot{\varepsilon}_{eff}^{cr} S_{ij} / \sigma_{eff}^{n_p}\end{aligned}\tag{7.1}$$

where ε_{eff} is the effective deformation and σ_{eff} is the effective stress.

The creep deformation rate is described by using the following approach for strain-hardening:

$$\dot{\varepsilon}_{cr} = f(\sigma_{eff}, \varepsilon_{cr}^V) = A_p \frac{\sigma_{eff}^{n_p}}{(\varepsilon^{V,0} + \varepsilon_{cr}^V)^\mu}\tag{7.2}$$

where A_p , n_p , and μ being material parameters.

Initially, the visco-plastic deformation rate depends more on those dislocations which are already present in the natural crystal (initial hardening $\varepsilon^{V,0}$). With further deformation, new

dislocations are generated which cause an increase in hardening. The formulation in equation 7.2 describes that the whole accumulated visco-plastic strain causes a material hardening. Therefore the hardening parameter and the total creep deformation ϵ_{cr} are equal. With further creep deformation the dislocation-density will increase which causes a decrease of the creep rate. (Fig. 7.9).

For determining the creep parameters, laboratory creep tests are required which are carried out over a long period without any dilatancy effect. With test periods of few months, recovery-processes play still no important roll. Thereby the creep behaviour can be described quite well with the strain-hardening approach as the comparison between the calculated and the measured values shows. (Fig. 7.1).

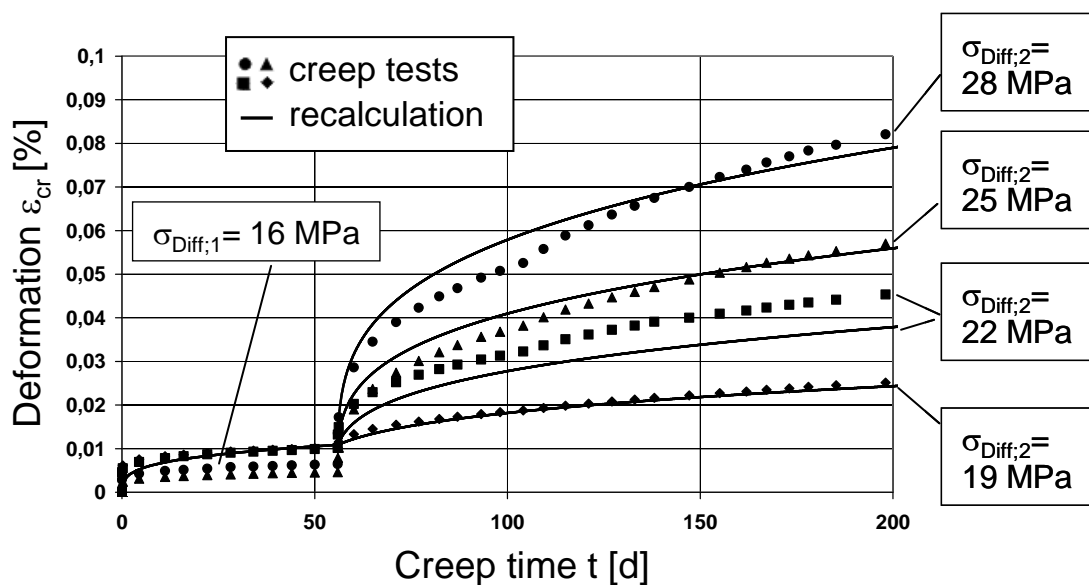


Figure 7.1: Creep tests carried out on Stassfurt-rock salt, Sondershausen mine, and recalculation with the creep parameters $A_p = 6,5 \cdot 10^{-24} [d^{-1}]$, $n_p = 11,88$, $\mu = 2,95$

This strain-hardening approach has been implemented in the FEM code MKEN and utilized for solving diverse rock mechanical problems (SALZER & SCHREINER 1991).

Those processes which cause a reduction of the existing intracrystalline dislocations are denoted as recovery which is counteracting the incremental material hardening. It is well known that the recovery is mainly a thermal activated process which runs quicker at higher temperatures. With growing density of dislocations, or hardening, also the recovery rate increases. Therefore the deformation part associated with the hardening, does no longer grow

with the same rate as the total deformation and tends finally to a saturation-value. Here, the creeping passes into its secondary (stationary) phase. Thus, when considering recovery in the creep approach, according to equation 7.3 the total creep rate $\dot{\epsilon}_{cr}$ is obtained from the share $\dot{\epsilon}_{cr}^V$ which increases hardening, and another share $\dot{\epsilon}_{cr}^E$ which describes recovery (SALZER, 1993).

$$\begin{aligned} \dot{\epsilon}_{cr} &= \dot{\epsilon}_{cr}^V + \dot{\epsilon}_{cr}^E \\ \text{and} & \\ \dot{\epsilon}_{cr}^V &= \dot{\epsilon}_{cr} - \dot{\epsilon}_{cr}^E \end{aligned} \tag{7.3}$$

For the recovery rate will be assumed:

$$\dot{\epsilon}_{cr}^E = \frac{\epsilon_{cr}^V}{t_0} \tag{7.4}$$

where t_0 is the recovery time.

At present, due to the diverse effects the recovery time t_0 cannot be derived from theoretical considerations. However, since recovery time has an essential effect on the stationary creep rate it is useful to determine that value by recalculation of the observed in-situ-behaviour. Also possible is the estimation of the recovery time based on the results of lab creep tests which are carried out over a long period. Regarding the laws of crystal physics which describe recovery in a first approximation it is appropriate to use the Arrhenius approach for introducing the temperature dependency of recovery time t_0 (SALZER ET AL. 1999).

$$t_0 = t_c \cdot e^{\frac{Q}{R \cdot T}} \tag{7.5}$$

where Q denotes the activation energy for the recovery process and t_c is a time constant. For room temperatures the recovery time is in the range from some years to several decades. When substituting in the creep approach of equation 7.2 the total deformation ϵ_{cr} by the accumulated hardening ϵ_{cr}^V so in the strain-hardening approach the recovery can be taken into consideration. The result is

$$\dot{\varepsilon}_{cr} = A_p \frac{\sigma_{eff}^{n_p}}{(\varepsilon^{V,0} + \varepsilon_{cr}^V)^\mu} \quad (7.6)$$

$$\dot{\varepsilon}_{cr}^V = A_p \frac{\sigma_{eff}^{n_p}}{(\varepsilon^{V,0} + \varepsilon_{cr}^V)^\mu} - \frac{\varepsilon_{cr}^V}{t_0}$$

In case of high values of hardening ε_{cr}^V recovery and hardening are in a dynamic equilibrium, i. e. the stationary creep phase is reached (Fig.7.10).

In a good approximation the pre-hardening $\varepsilon^{V,0}$ can set to zero. For the hardening rate in the stationary state the expression $\dot{\varepsilon}_{cr,S}^V = 0$ applies which results in :

$$0 = \dot{\varepsilon}_{cr} - \dot{\varepsilon}_{cr}^E \quad \Rightarrow \quad \dot{\varepsilon}_{cr} = \dot{\varepsilon}_{cr}^E$$

$$A_p \frac{\sigma_{eff}^{n_p}}{\varepsilon_{cr}^{V\mu}} = \frac{\varepsilon_{cr}^V}{t_0} \quad (7.7a)$$

$$\varepsilon_{cr,S}^V = \left(A_p \cdot t_0 \cdot \sigma_{eff}^{n_p} \right)^{\frac{1}{1+\mu}}$$

By substituting equation 7.7a into equation 7.2 the pre-factor A_s and the stress exponent n_s for stationary creep (power law) are obtained as

$$\dot{\varepsilon}_{cr,S} = A_s \cdot \sigma_{eff}^{n_s} \quad \rightarrow \quad \varepsilon^{V,0} = 0 \quad (7.7b)$$

$$\text{with: } A_s = A_p \left(\frac{1}{A_p \cdot t_0} \right)^{\frac{\mu}{1+\mu}} \quad \text{and} \quad n_s = \frac{n_p}{1+\mu}$$

When the temperature dependent recovery time t_0 according to equation 7.5 is taken into consideration the temperature dependency for creep is calculated as follows:

$$A_s = A_p \left(\frac{1}{A_p \cdot t_0} \right)^{\frac{\mu}{1+\mu}} \cdot e^{-\frac{Q(1+\mu)}{\mu \cdot R \cdot T}} \quad (7.8)$$

Consideration of damage

(GÜNTHER & SALZER 2007, GÜNTHER 2009)

In triaxial compression tests the test specimen is compressed under a constant load rate. For this purpose, load is increased permanently until fracture occurs. Thereby existing dislocations are activated and new ones are generated, which, due to the growing dislocation density, causes an increase of hardening and consequently of the strength too. Because of the short test periods the recovery of dislocations does not play any substantial role. At the same time more and more dislocation pile-ups develop, which counteract increasingly the deformation. Consequently, in the domain of the dislocation pile-ups, increased local stresses will develop which cause the generation of microcracks and progressive damage, at loads beyond the dilatancy boundary.

In laboratory tests, the growing damage can be measured as a volume increase (dilatancy). The dilatancy-boundary describes that stress level at which an increase of the specimen volume is measured first.

Because the damage counteracts the hardening the material becomes more and more ductile. Under consideration that deformation part $\dot{\epsilon}_{cr}^S$ which characterizes the damaging process and strain softening, resp., (in the following briefly denoted as damage) equation 7.3 yields:

$$\dot{\epsilon}_{cr}^V = \dot{\epsilon}_{cr} - \dot{\epsilon}_{cr}^E - \dot{\epsilon}_{cr}^S$$

and

$$\dot{\epsilon}_{cr}^V = \dot{\epsilon}_{cr} - \dot{\epsilon}_{cr}^S \quad \text{for } \dot{\epsilon}_{cr}^E \rightarrow 0 \tag{7.9}$$

Here, in the case of triaxial compressive short term tests, the recovery can be neglected at room temperature. That means when damage rate $\dot{\epsilon}_{cr}^S$ and creep rate $\dot{\epsilon}_{cr}$ become equal, then the material hardening and the strength respective become constant. The generation of dislocations and the damage (or microcrack) evolution are in equilibrium with regard to their effects. At this state the material is in the yielding point with ideal plasticity behaviour. Consequently, the peak strength is obtained if the salt is no longer subject to deformation hardening, i. e. when the effective hardening rate $\dot{\epsilon}_{eff}^V$ is equal to zero (eq. 7.10). A classical strength criterion (yield function) is not required anymore.

$$\dot{\epsilon}_{cr}^V = \dot{\epsilon}_{cr} - \dot{\epsilon}_{cr}^S = 0 \quad \Rightarrow \quad \sigma_{eff} = \sigma_{eff, Max} \quad (7.10)$$

When the damaging rate $\dot{\epsilon}_{cr}^S$ exceeds the creep rate $\dot{\epsilon}_{cr}$ then the effective hardening rate $\dot{\epsilon}_{cr}^V$ becomes negative and the material softens. The strength is now in the post-failure region.

In Figure 7.2 the trace of the dilatancy rate $\dot{\epsilon}_{vol}$ as measured in the triaxial test has been plotted versus the axial deformation ϵ_1 and as comparison additionally the externally impressed deformation rate of the triaxial test (with $\dot{\epsilon}_1 = 10^{-5} s^{-1}$) and also the measured trace of strength. It can be seen, that in the pre-failure region the dilatancy rate $\dot{\epsilon}_{vol}$ is significantly below the deformation rate and rises in a comparatively uniform manner along with the deformation. In the region of peak strength the dilatancy rate $\dot{\epsilon}_{vol}$ reaches the value of the deformation rate and begins to rise in an over-proportionate manner. This acceleration is linked with the phenomenon of coalescence of microcracks to macrocracks. In the first third of the post-failure region this process is terminated by the fact that the dilatancy rate reaches its maximum value.

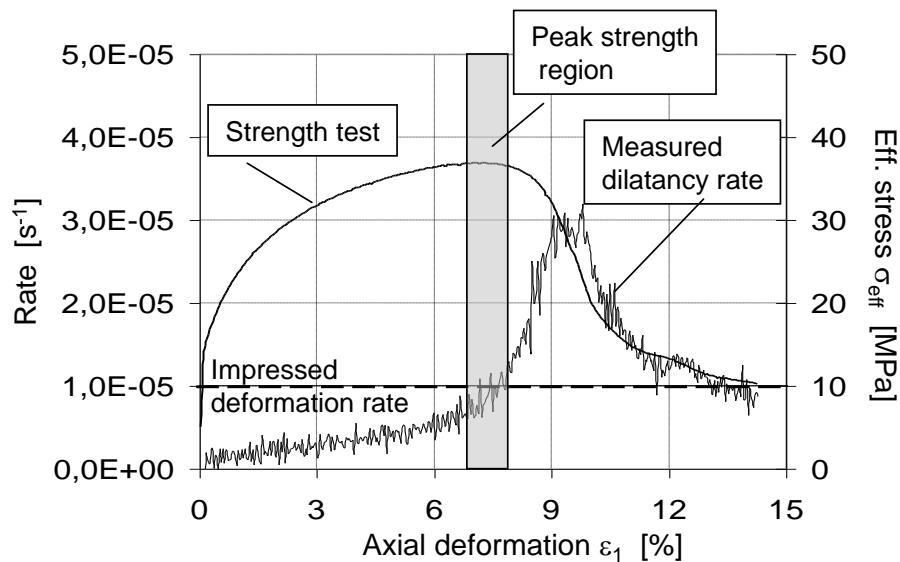


Figure 7.2: Triaxial test, measured deformation rate and dilatancy rate

In principle, the effects as represented in Figure 7.2 can be observed in all triaxial tests which have been investigated. In the constitutive model, this behaviour is taken into consideration in that way that the effective hardening rate $\dot{\epsilon}_{cr}^V$ is lowered by the dilatancy rate $\dot{\epsilon}_{vol}$. Therefore,

in the creep approach the damage rate $\dot{\varepsilon}_{cr}^S$ in equation 7.9 is replaced by the dilatancy rate $\dot{\varepsilon}_{Vol}$

$$\dot{\varepsilon}_{cr}^V = \dot{\varepsilon}_{cr} - \dot{\varepsilon}_{cr}^E - \dot{\varepsilon}_{Vol} \quad (7.11)$$

The material strength is the measurable resistance which a material opposes to plastic deformation resp. failure. In the constitutive model this causal relationship is described by the current effective hardening ε_{cr}^V an internal state variable, which determines the visco-plastic behaviour. Therefore, a formulation of the strength by a failure criterion is not required. It is replaced by the description of the dilatancy behaviour.

Dilatancy as function of the damage work and the minimum stress

(GÜNTHER & SALZER 2007, GÜNTHER 2009)

In the constitutive model the dilatancy is described as a function of the minimum stress σ_3 and the specific deformation work above the dilatancy boundary $\dot{\varepsilon}_{Vol} = f(\sigma_3, U)$. Here, the specific deformation work above the dilatancy boundary U_{Dil} (in the following briefly denoted as damage work) is defined as follows:

$$\begin{aligned} \Delta U_{Dil} &= (\sigma_{eff} - \sigma_{eff}^{Dil}) \cdot \Delta \varepsilon_{cr} \\ U_{Dil} &= \int (\sigma_{eff} - \sigma_{eff}^{Dil}) \cdot d\varepsilon_{cr} \end{aligned} \quad (7.12)$$

Many tests have shown that dilatancy boundary and residual strength can approximately be equated one to the other. This allows to describe the damage work according to equation 7.12 in a simple manner and to ensure that the calculated final value of softening tends towards the value of the residual strength. In the constitutive model the dilatancy boundary σ_{eff}^{Dil} is described as follows (Fig. 7.3):

$$\sigma_{eff}^{Dil}(\sigma_3) = \sigma_3 \cdot \left[\frac{D_1}{D_2 + \sigma_3} + D_3 \right] \quad (7.13)$$

wherein for the Stassfurt rock salt the following parameters have been determined:

Table 7.1: Parameters of the dilatancy boundary function 7.13

Staßfurt rock salt (Na2)	D1 [MPa]	D2 [MPa]	D3 [MPa]
Sondershausen salt mine	12	0,05	2
Asse site	8	0,25	4,8

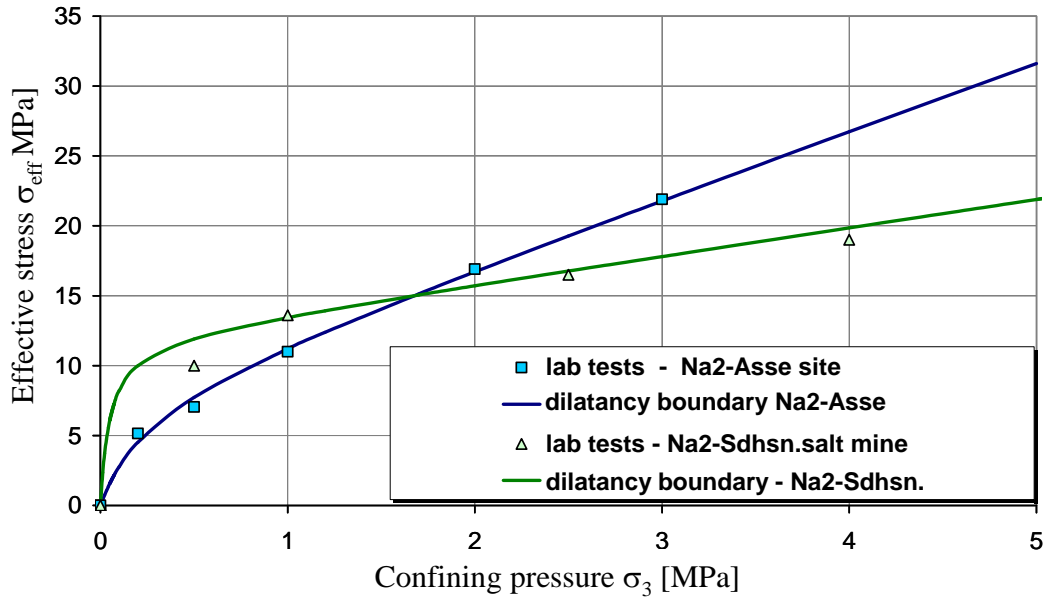


Figure 7.3: Dilatancy boundary for the Staßfurt rock salt from the Sondershausen mine

When plotting the measured dilatancy ε_{Vol} in dependency of the damage work U_{Dil} in a diagram (Fig. 7.4), so the following functional relationship between these two quantities appears:

$$\varepsilon_{\text{Vol}}(U_{\text{Dil}}) = A_1 \cdot U_{\text{Dil}} + \frac{A_2}{A_3} \cdot \exp[A_3 \cdot U_{\text{Dil}}] \quad (7.14)$$

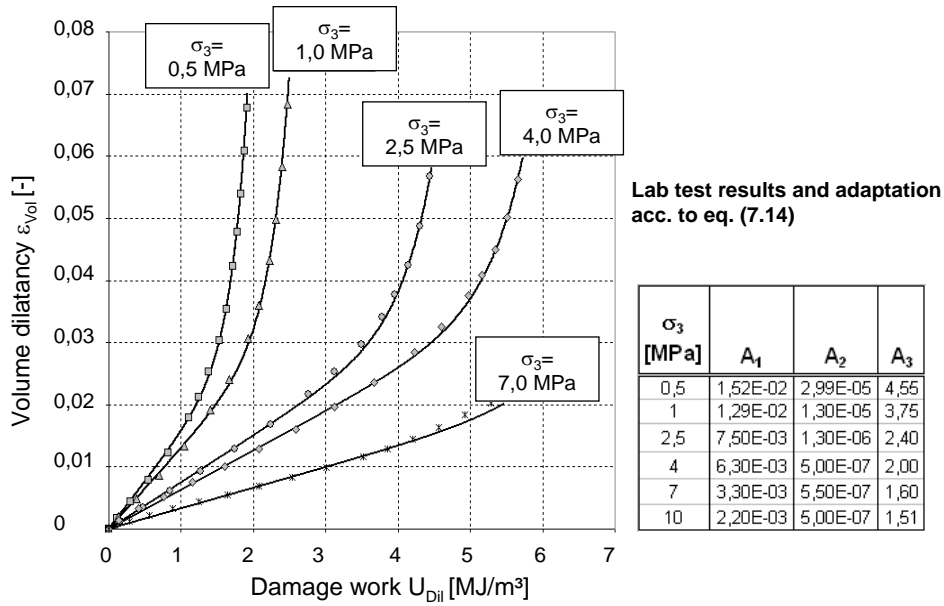


Figure 7.4: Relationship between dilatancy ε_{Vol} and damage work U_{Dil} ; Sonderhausen salt mine - adaptation to tests

Depending on the confining pressure σ_3 different curve parameters A_1 , A_2 , and A_3 (Fig. 7.4) will be obtained which, in a good approximation, can be described as exponential functions of σ_3 given below.

$$\begin{aligned}
 A_1 &= f(\sigma_3) = a_1 + a_2 \cdot \exp[a_3 \cdot \sigma_3] \\
 A_2 &= f(\sigma_3) = a_4 + a_5 \cdot \exp[a_6 \cdot \sigma_3] \\
 A_3 &= f(\sigma_3) = a_7 + a_8 \cdot \exp[a_9 \cdot \sigma_3] \quad a_1 \dots a_9 [\text{MPa}]^{-1}
 \end{aligned} \tag{7.15}$$

The following parameters have been derived:

Stassfurt rock salt from the Sondershausen salt mine:

$$A_1(\sigma_3) \Rightarrow \begin{cases} a_1 = 2,1 \cdot 10^{-3} \\ a_2 = 0,016 \\ a_3 = -0,39 \end{cases} ; \quad A_2(\sigma_3) \Rightarrow \begin{cases} a_4 = 5 \cdot 10^{-7} \\ a_5 = 8 \cdot 10^{-5} \\ a_6 = -2 \end{cases} ; \quad A_3(\sigma_3) \Rightarrow \begin{cases} a_7 = 1,5 \\ a_8 = 4,15 \\ a_9 = -0,6 \end{cases}$$

Stassfurt rock salt from the Asse site:

$$A_1(\sigma_3) \Rightarrow \begin{cases} a_1 = 5,0 \cdot 10^{-3} \\ a_2 = 0,0135 \\ a_3 = -0,4 \end{cases}; \quad A_2(\sigma_3) \Rightarrow \begin{cases} a_4 = 1 \cdot 10^{-6} \\ a_5 = 2,5 \cdot 10^{-4} \\ a_6 = -6,25 \end{cases}; \quad A_3(\sigma_3) \Rightarrow \begin{cases} a_7 = 0,0 \\ a_8 = 5,13 \\ a_9 = -0,3 \end{cases}$$

After substituting equation 7.15 into equation 7.14 also the dependency on the minimum principal stress σ_3 is obtained:

$$\varepsilon_{\text{vol}}(U_{\text{Dil}}, \sigma_3) = A_1(\sigma_3) \cdot U_{\text{Dil}} + \frac{A_2(\sigma_3)}{A_3(\sigma_3)} \cdot \exp[A_3(\sigma_3) \cdot U_{\text{Dil}}] \quad (7.16)$$

By derivative of the equation 7.16 with respect to U_{Dil} the incremental increase of the dilatancy as a function of the accumulated damage work and the minimum principal stress is calculated as:

$$\frac{d\varepsilon_{\text{vol}}}{dU_{\text{Dil}}} = A_1(\sigma_3) + A_2(\sigma_3) \cdot \exp[A_3(\sigma_3) \cdot U_{\text{Dil}}] \quad (7.17a)$$

In the numerical implementation the change in dilatancy in finite time steps corresponds to the increase multiplied by the change of work in the respective time step:

$$\frac{\Delta\varepsilon_{\text{vol}}}{\Delta t} = \dot{\varepsilon}_{\text{vol}} = [A_1(\sigma_3) + A_2(\sigma_3) \cdot \exp[A_3(\sigma_3) \cdot U_{\text{Dil}}]] \cdot \frac{\Delta U_{\text{Dil}}}{\Delta t} \quad (7.17b)$$

In creep-tests with constant loading above the dilatancy boundary $\sigma_{\text{eff}}^{\text{Dil}}$ the described approach causes that depending on the accumulated damage work U_{Dil} effective hardening $\varepsilon_{\text{cr}}^{\text{V}}$ is gradually reduced. Resulting from that, the material passes finally into the tertiary creep phase. Figure 7.5 illustrates to it the recalculation of a creep test including creep failure for Asse rock salt.

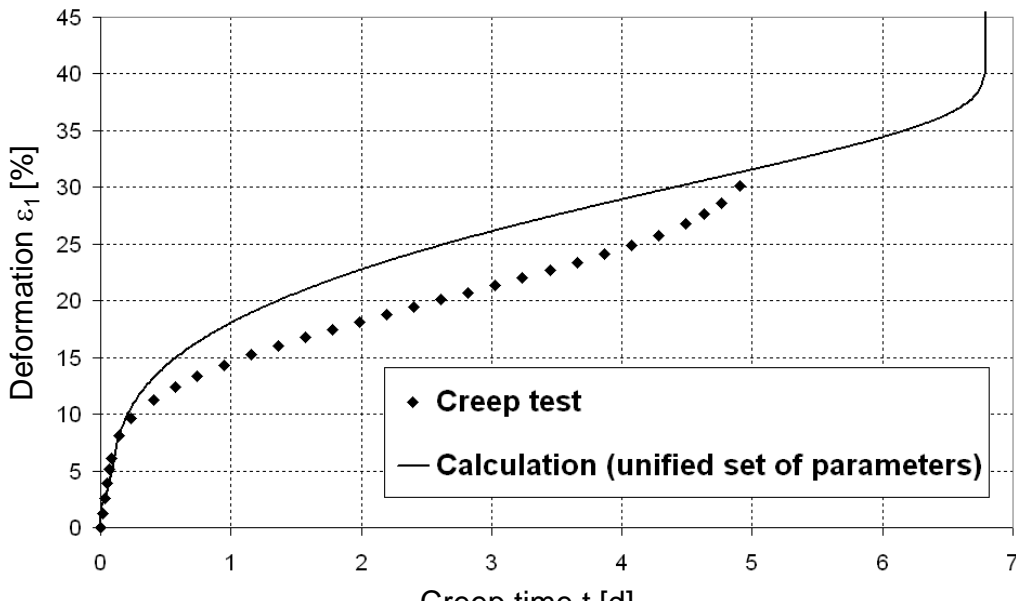


Figure 7.5: Creep test with creep failure and recalculation with the constitutive model - Stassfurtsteinsalz Na2 from the Asse site

Modified stress exponent in the dilatancy region

(GÜNTHER & SALZER 2007, GÜNTHER 2009)

From recalculation of the triaxial tests with constant deformation follows that within the dilatancy region the stress exponent n_p of the creep model depends on both the minimum stress and the dilatancy in the following form:

$$n_p = f(\sigma_3, \varepsilon_{Vol}) = \frac{n_{\varepsilon_{Vol}0} + n_1 \cdot \exp[n_2 \cdot \sigma_3] \cdot [1 - \exp(-n_3 \cdot \varepsilon_{Vol})]}{(1 - \varepsilon_{Vol})^{n_4}} \quad (7.18)$$

where $n_{\varepsilon_{Vol}0}$ denotes the stress exponent for the non-damaged material. This exponent can be derived from creep tests carried out in the stress space below the dilatancy boundary. The other material parameters must be determined by way of stepwise calibration to approximate to the test results of the triaxial compressive tests. In this case, for the Stassfurt rock salt The following values have been determined:

Table 7.2: Parameters for equation 7.18

Stauffurt rock salt (Na2) from:	$n_{\varepsilon_{Vol} < 0}$	n_1	n_2	n_3	n_4
Sondershausen salt mine	11,88	0,55	-0,18	2000	0,5
Asse site	15,18	0,8	-0,33	2000	0,5

Recalculations of the triaxial tests prove (Fig. 7.6– left picture) that in consideration of the equation 7.18 the strength and deformation behaviour of ductile salt rock can be calculated in a very good approximation. The same can be stated with respect to the description of the behaviour of dilatancy (Fig. 7.6 – right picture).

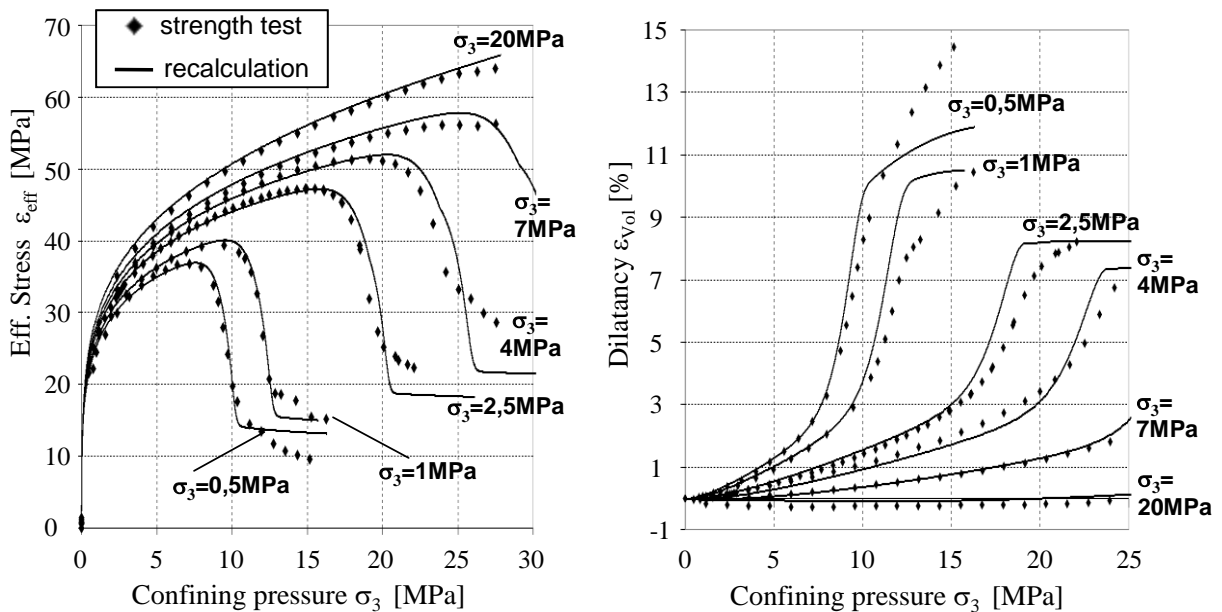


Figure 7.6: Comparison between calculated and measured strength behaviour and comparison between calculated and measured dilatancy behaviour for Stauffurteinstsalz Na2 from the Sondershausen salt mine

In the constitutive model the strength and dilatancy behaviour is determined by the accumulated damage work U_{Dil} . Under low deformation rates the part of the total deformation without damage is growing whereas the deformation rate is high the part of damage is quite high. Therefore, in the constitutive model the ratio between the deformation parts which are induced by damage and those free of damage depends on the deformation rate too. Since hardening is determining the strength, the concept of the accumulated damage work U_{Dil} results in a strength and dilatancy behaviour which depends on the loading rate so that the short-time strength as determined in the fast triaxial test as well as the lower long-time strength can be

Figure 7.7 demonstrates a comparison between the measured strength behaviour and that which has been calculated on the basis of the constitutive model at different deformation rates. In Figure 7.8 the respective dilatancy behaviour is represented. The comparison shows that at different deformation rates the constitutive model allows to simulate the measured strength and dilatancy behaviour quite well.

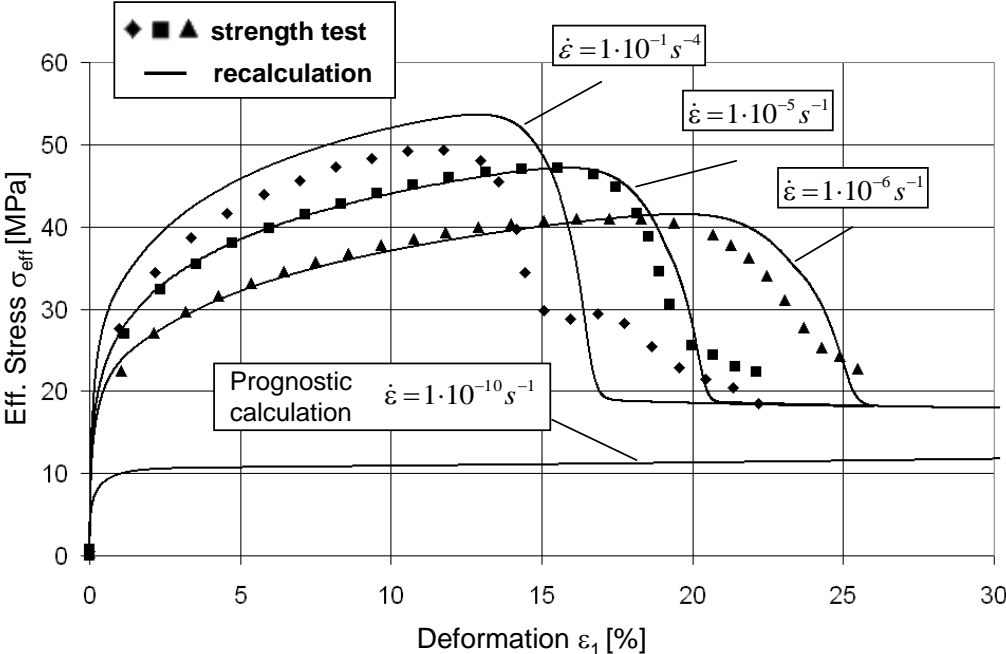


Figure 7.7: Comparison between calculated and measured strength behaviour under different loading rates (confinement pressure $\sigma_3 = 2,5 \text{ MPa}$)

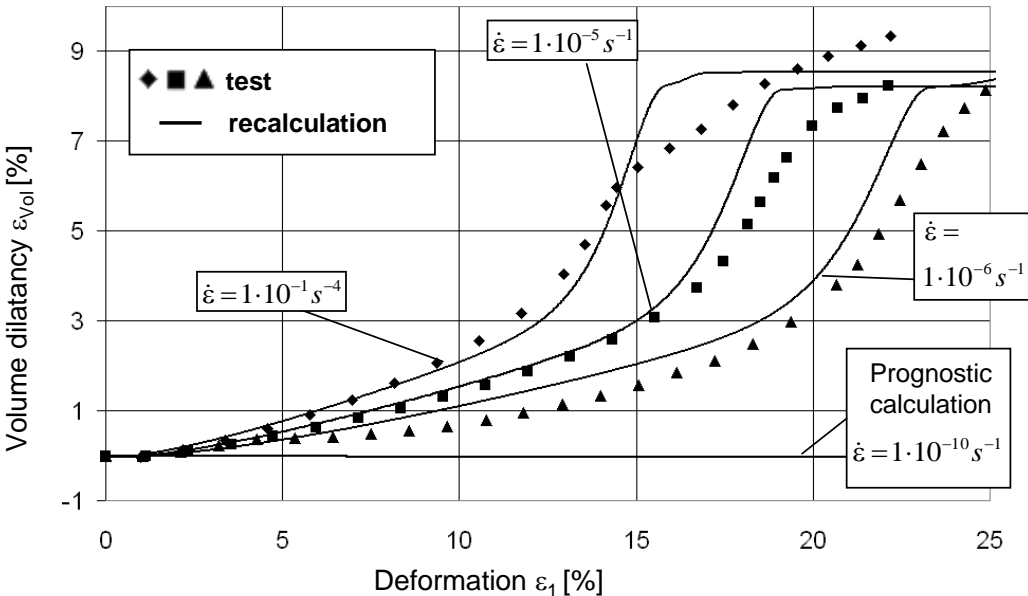


Figure 7.8: Comparison between calculated and measured dilatancy behaviour under different loading rates (confinement pressure $\sigma_3 = 2,5 \text{ MPa}$)

To illustrate an important consequence which may be drawn from the presented relationships, in addition a prognostic calculation has been carried out using a deformation rate of $\dot{\varepsilon} = 1 \cdot 10^{-10} \text{s}^{-1}$ which is typical of the conditions found in situ (prognostic calculation curve in Fig. 7.7). Due to this low deformation rate in the predicted test ($\sigma_3 = 2,5 \text{MPa}$) no stresses develop which exceed the dilatancy boundary ($\sigma_{\text{eff}}^{\text{Dil}}(\sigma_3 = 2,5 \text{MPa}) = 17 \text{MPa}$). Therefore, at this rate and at the given confining pressure the deformation is free of damage, i. e. creeping without any dilatancy (Fig. 7.8 - prognostic calculation curve).

Elastic constants under dilatancy and stress correction

(GÜNTHER & SALZER 2007, GÜNTHER 2009)

As a result of the dilatant loosening-up also the elastic behaviour of the rock body alters so that with increasing damage its compressibility increases and the Poisson's ratio ν tends towards the value of $\nu \rightarrow 0,5$. In non-damaged and non-loosened rock elements the well known relationships with respect to E (young modulus) and ν apply for the compression modulus K and for the shear modulus G .

$$K = \frac{E}{3 \cdot (1 - 2\nu)}$$

$$G = \frac{E}{2 \cdot (1 + \nu)}$$
(7.19)

To describe the elastic parameters under consideration of the dilatancy the following empirical relationships provide a practical description:

$$K(\varepsilon_{\text{Vol}}) = \frac{K_0 - K_R}{(1 + \varepsilon_{\text{Vol}})^\alpha} + K_R$$

$$\nu(\varepsilon_{\text{Vol}}) = \frac{\nu_0 - \nu_R}{(1 + \varepsilon_{\text{Vol}})^\alpha} + \nu_R$$
(7.20)

where K_0 - compression modulus for non-damaged salt,

K_R - compression modulus in the region of residual strength

ν_0 - Poisson's ratio for non-damaged salt

ν_R - Poisson's ratio in the region of residual strength and
 α - parameter of curvature.

These equations 7.19 and 7.20 allow calculating the dilatancy-depending shear modulus:

$$G(\varepsilon_{Vol}) = \frac{3}{2} K(\varepsilon_{Vol}) \cdot \frac{1 - 2 \cdot \nu(\varepsilon_{Vol})}{1 + \nu(\varepsilon_{Vol})} \quad (7.21)$$

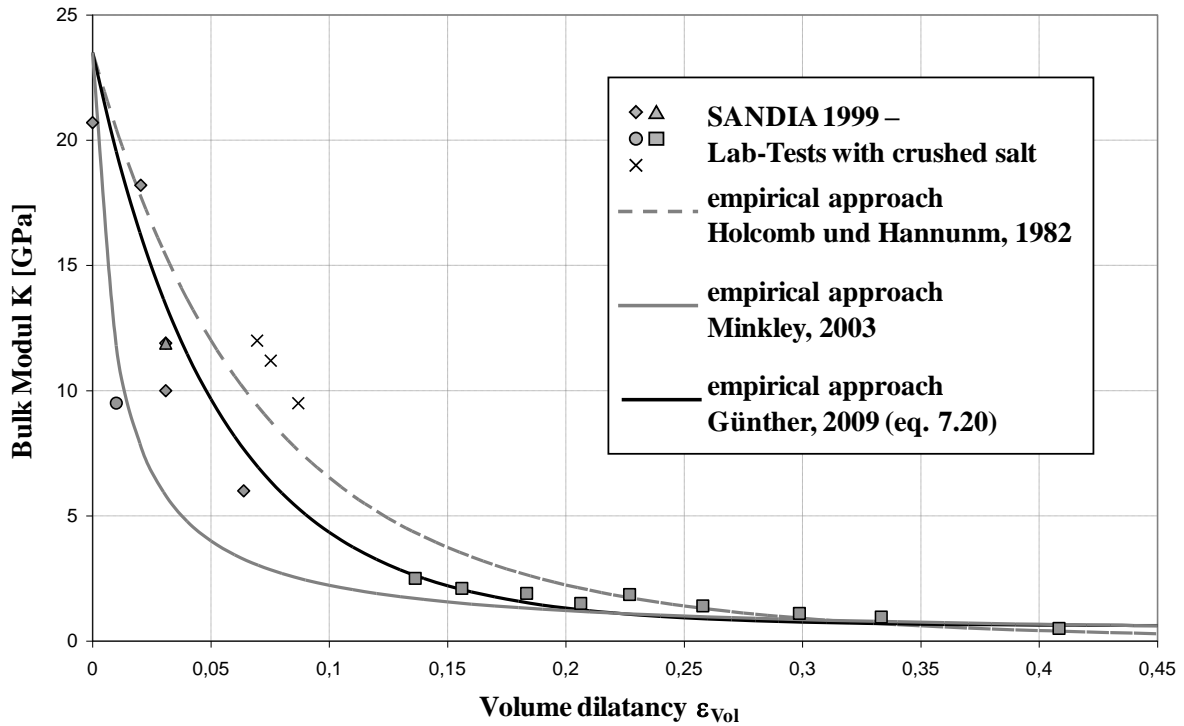


Figure 7.9: Reduction of the bulk modulus as function of the dilatancy (according eq. 7.20)

Figure 7.9 shows that the description according eq. 7.20 is similar to other approaches published in the international literature.

In the calculation the elastic volume change results the octahedral normal stress $\Delta\sigma_0$.

$$\Delta\sigma_0 = K \cdot \Delta\varepsilon_{Vol}^e \quad (7.22)$$

By the influence of the dilatancy the compression modulus changes according to equation 7.20. In addition, the damage-induced volume increase $\Delta\varepsilon_{Vol}$ as calculated according to

equation 7.17b counteracts the elastic volumetric compaction $\Delta\varepsilon_{\text{Vol}}^e$. Both, the dilatancy-depending compression modulus $K(\varepsilon_{\text{Vol}})$ and the damage-induced volume increase $\Delta\varepsilon_{\text{Vol}}$ in equation 7.22 need to be taken into account in correcting the octahedral normal stress by alteration of the stress state. As a result of both, the accumulated (ε_{Vol}) and incremental ($\Delta\varepsilon_{\text{Vol}}$) volume increase, the correction is obtained according to the following equation:

$$\Delta\sigma_0 = K(\varepsilon_{\text{Vol}}) \cdot (\Delta\varepsilon_{\text{Vol}}^e - \Delta\varepsilon_{\text{Vol}}) \quad (7.23)$$

Conclusions

The presented constitutive model describes the mechanical behaviour of rock salt in a good approximation comprehensively within the scope of a unified creep approach where the hardening has been implemented as an interior state variable. Here, hardening is determined by the processes of migration and generation of dislocations and their recovery on one hand and by those of damage on the other one. These crystal-physical processes that are governing the mechanical behaviour of the salt rocks form the theoretical base for the formulation of the constitutive model. In the following the individual contribution of the various effects which have been integrated into the constitutive model are demonstrated in synoptic figures referring exemplarily to a hypothetic creep test.

In the region of primary creep below the dilatancy boundary the hardening-parameter $\varepsilon_{\text{cr}}^V$ and the accumulated creep deformation ε_{cr} are equal. (Fig. 7.10).

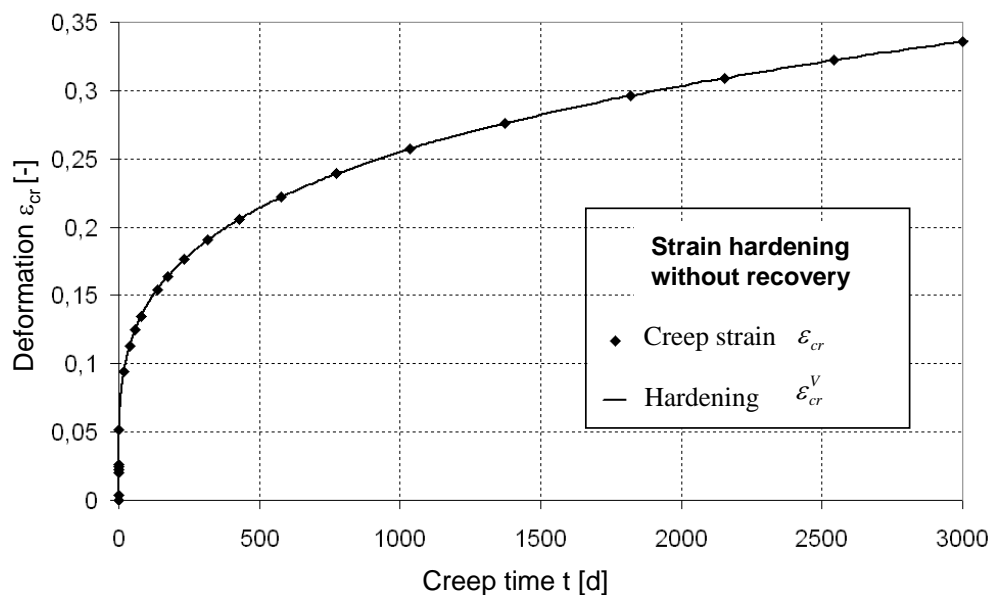


Figure 7.10: Modelling of creep deformation – exemplary behaviour (only strain-hardening without recovery and damage/dilatancy).

Over longer periods of time and for higher temperatures the recovery acts in a hardening-reducing manner so that finally a dynamic equilibrium between hardening and recovery establishes, i. e. the hardening parameter ε_{cr}^V tends to a constant value and the phase of stationary creep is reached (Fig. 7.11).

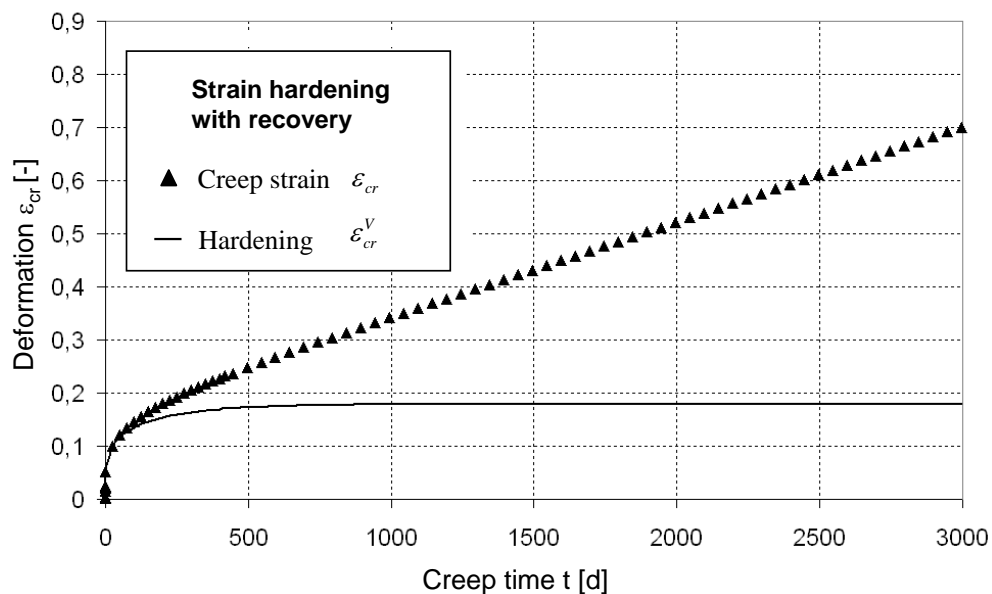


Figure 7.11: Modelling of creep deformation – exemplary behaviour (strain-hardening with recovery but without damage/dilatancy).

If creep occurs in the stress space above the dilatancy boundary micro cracking evolves, whereby the progressive damage leads to a reduction of the hardening

Analyses of triaxial strength tests have demonstrated that the hardening-reducing effect of damage can be equated to the measured dilatancy. The latter can be described as a function of both, the specific deformation work performed above the dilatancy boundary (damage work) and the minimum stress. Both influence parameters have to be determined by means of triaxial tests. Finally, in creep tests the reduction of the hardening ε_{cr}^V along with growing damage and dilatancy, resp., results in an accelerated creep and in creep failure, resp. (Fig. 7.12).

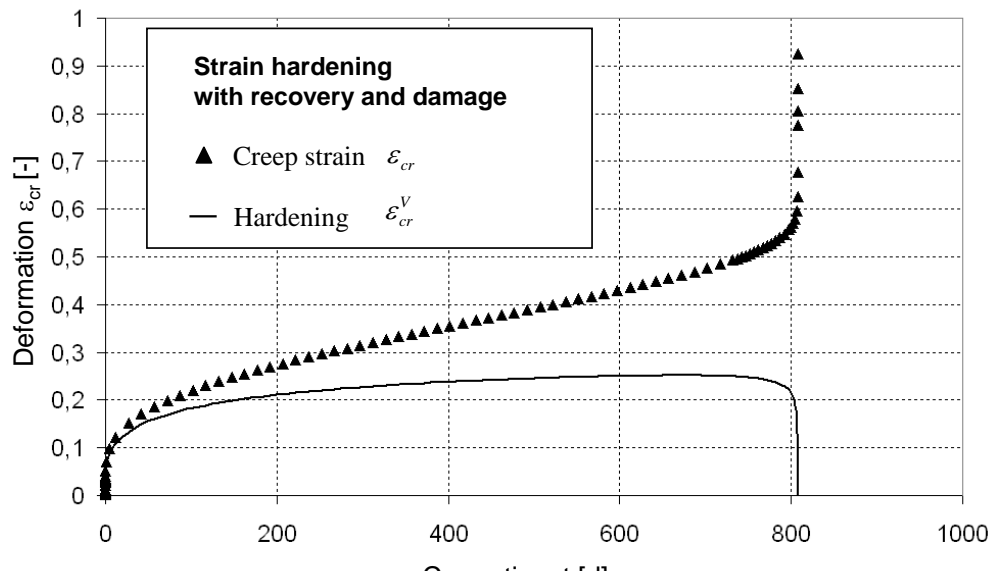


Figure 7.12: Modelling of creep deformation – exemplary behaviour (strain-hardening with recovery and damage/dilatancy).

Literature:

BLUM, W., 1978: *Gleitung und Erholung während plastischer Verformung kristalliner Stoffe bei hoher Temperatur*. Habilitationsschrift, Universität Erlangen-Nürnberg.

Günther, R.-M, Salzer, K., 2007: *A model for rock salt, describing transient, stationary, and accelerated creep and dilatancy*.- In: *The mechanical behaviour of salt; Proc. of the sixth conf.*, S.109-117, publ. by Taylor& Francis/ Balkema, 2007, ISBN: 978-0-415-44398-2, 2007

Günther, R.-M, 2009: *Erweiterter Dehnungs-Verfestigungs-Ansatz, Phänomenologisches Stoffmodell für duktile Salzgesteine zur Beschreibung primären, sekundären und tertiären Kriechens*. Veröffentlichungen des Institutes für Geotechnik der TU Bergakademie Freiberg, Heft 2009-4.

ITASCA: *FLAC 4.0 – Fast Lagrangian Analysis of Continua. Version 4.0. User's Manual*, ITASCA Consulting Group Inc., Minneapolis, Minnesota, USA, 2000.

MENZEL, W., SCHREINER W., 1977: *Zum geomechanischen Verhalten von Steinsalz verschiedener Lagerstätten der DDR Teil II: Das Verformungsverhalten*. Neue Bergbautechnik, Heft 8, 7.Jg., März 1977.

ODQVIST, F. K. G., HULT, H., 1962: *Kriechfestigkeit metallischer Werkstoffe*. Springer Verlag, Berlin.

SALZER, K, SCHREINER, W.: *Der Rechencode MKEN zur Ermittlung der Zeitabhängigkeit des Spannungs-Verformungszustandes um Hohlräume im Salzgebirge*. Kali und Steinsalz, Band 10, Heft 12, Oktober 1991.

SALZER, K.: *Ableitung eines kombinierten Kriechgesetzes unter Berücksichtigung der Erholung*. Teilbericht zum BMFT Vorhaben 02 C 00 628, IfG Leipzig, 1993.

SALZER, K., KONIETZKY, H., GÜNTHER, R.-M.: *A new Creep Law to describe the transient and secondary Creep Phase*. Proceedings of the 4th European Conference on Numerical Methods in Geotechnical Engineering NUMGE98, Udine, 14.-16. 10. 1998, 788 Seiten, ISBN-13: 978-3211831410, Springer-Verlag, Wien, 1999.

HUNSCHE U.: *Determination of the Dilatancy Boundary and Damage up to Failure for four types of Rock Salt at different Stress Geometries*. In: *The Mechanical Behavior of Salt IV; Proceedings of the 4th Conference*, Montreal, 1996, S. 163-174, ISBN-13: 978-3540290346, TTP Trans Tech Publications, Clausthal 1998.